This is an open access article published under an ACS AuthorChoice License, which permits copying and redistribution of the article or any adaptations for non-commercial purposes.

ACS OMEGA

Article

http://pubs.acs.org/journal/acsodf

Selective Adsorption of Coronene atop the Polycyclic Aromatic Diimide Monolayer Investigated by STM and DFT

Yanfang Geng,[†,§] Shuai Wang,[†,§] Mengqi Shen,[†] Ranran Wang,[‡] Xiao Yang,[‡] Bin Tu,*[,†] Dahui Zhao,*[,‡] and Qingdao Zeng*[,†]

[†]CAS Key Laboratory of Standardization and Measurement for Nanotechnology, CAS Center for Excellence in Nanoscience, National Center for Nanoscience and Technology (NCNST), 11 Zhongguancunbeiyitiao, Beijing 100190, P. R. China

[‡]Beijing National Laboratory for Molecular Sciences, The Key Laboratory of Polymer Chemistry and Physics of the Ministry of Education, College of Chemistry, Peking University, Beijing 100871, P. R. China

Supporting Information

ABSTRACT: The self-assemblies of polycyclic aromatic diimide (PAI) compounds on solid surfaces have attracted great interest because of the versatile and attractive properties for application in organic electronics. Here, a planar guest species (coronene) selectively adsorbs on the helicene-typed PAI1 monolayer strongly, depending on the conjugated cores of these PAIs. PAI1 molecule displays evidently a bowl structure lying on the highly oriented pyrolytic graphite surface due to the torsion of the "C"-shaped fused benzene rings. In combination with density functional theory calculation, the selective inclusion of coronene atop the backbone of the PAI1 array might be attributed to the bowl structure, which provides a groove for immobilizing coronene molecules. On the other planar densely packed arrays, it is difficult to observe the unstable adsorption of coronene. The selective addition of coronene molecules would be a strategic step toward the controllable multicomponent supramolecular architectures.

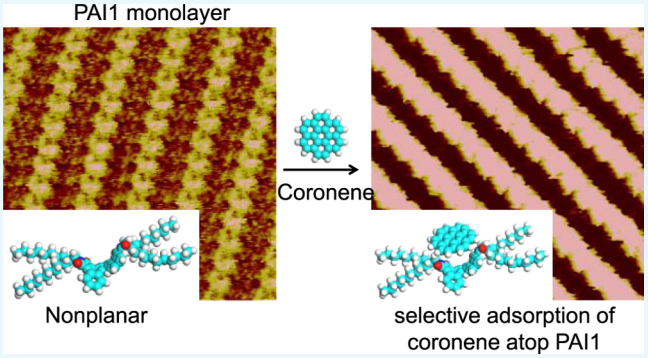

INTRODUCTION

Two-dimensional (2D) self-assemblies on a solid surface are an interesting subject due to the promising perspectives in the nanotechnology field.[1−3] Although the exploitation of controlled supramolecular chemistry has reached a maturity level where the specific self-assembly can be predicted to high accuracy, controllable ordering in the multicomponent architectures at the molecular scale remains a challenge. To obtain well-defined complex structures, 2D multicomponent nanostructures through the selective accommodation of many types of guest molecules in various host template networks have attracted a great deal of attention over the past decades.[4,5] In most cases, the host molecules formed 2D solid networks with suitable cavities for guest molecules, and the inclusion of guest molecules cannot disturb the already existing host network. The shape and size complementarities between the cavity and guest molecule play an important role in the nanostructure. On the other hand, there are a few cases of coassembly in which host nanostructures on the solid surface were tuned by the inclusion of guest molecules.[6,7] The applications of host−guest systems for the fixation of functional compounds have been hampered by the inefficient understanding of the behavior of incorporation of guest species on the host molecules.

Among the most studied guest molecules, coronene (Cor), with sixfold symmetry, displayed a stable adsorption structure on unmodified solid surfaces, including various metal surfaces[8,9] and the highly oriented pyrolytic graphite (HOPG) substrate.[10−12] In most reports, a single coronene molecule or clusters were confined within various networks.[13−27] Note that the uses of coronene to transform the self-assembled surface structures have also been observed.[16,17,19] In addition to the location of coronene in the host cavity, there are some cases in which coronene molecules are partly or completely located on the host molecules. Horn et al. found an ordered second coronene layer on top of the first coronene layer due to the coronene layer and substrate underneath.[28,29] Zhang et al. observed a coronene layer on top of HPB-6pa network, which might be attributed to the electronic interaction and van der Waals interactions.[30] Note that the cavity of HPB-6a is slightly smaller than the size of the coronene molecule by around 0.12 nm. Therefore, the adsorption site of coronene might be attributed to many factors, like the substrate, the cavity of host network, the host structure, and so on.

In this study, we designed four polycyclic aromatic diimide (PAI) derivatives, namely, PAI1 (*N*,*N*′-di(2-octyldodecyl)-dibenzo[*c*,*g*]phenanthrene-1,2,5,6-tetracarboxyldiimide), PAI2 (*N*,*N*′-di(2-octyldodecyl)benzo[*k*]tetraphene-5,6,12,13-tetra-

Received: June 29, 2017
Accepted: August 25, 2017
Published: September 8, 2017

 © 2017 American Chemical Society

DOI: 10.1021/acsomega.7b00891
ACS Omega 2017, 2, 5611−5617

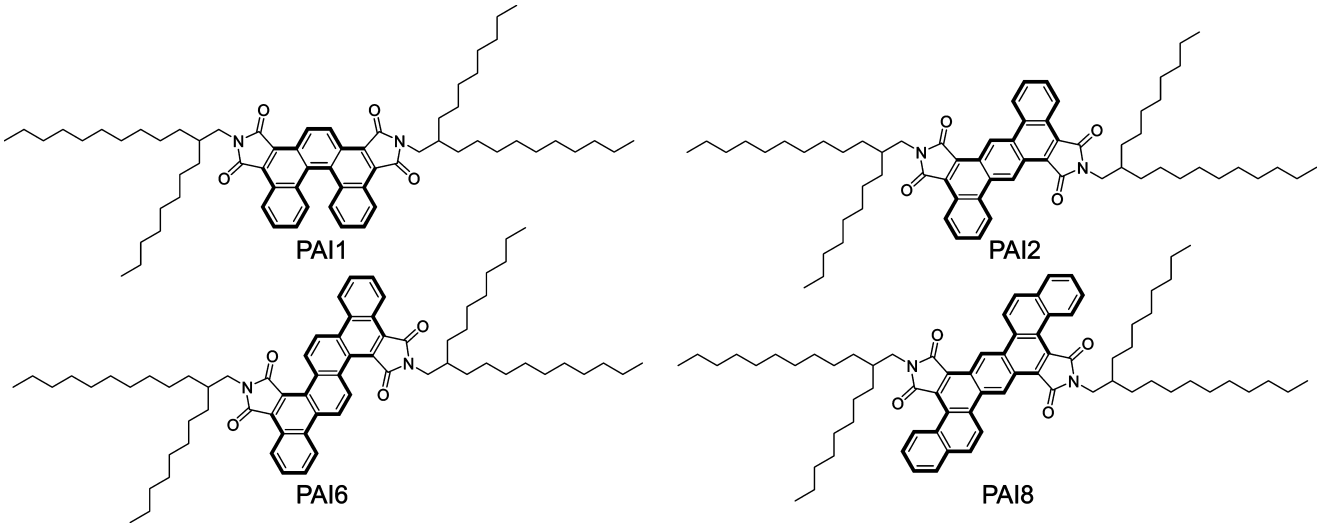

Figure 1. Chemical structures of four PAI-based compounds.

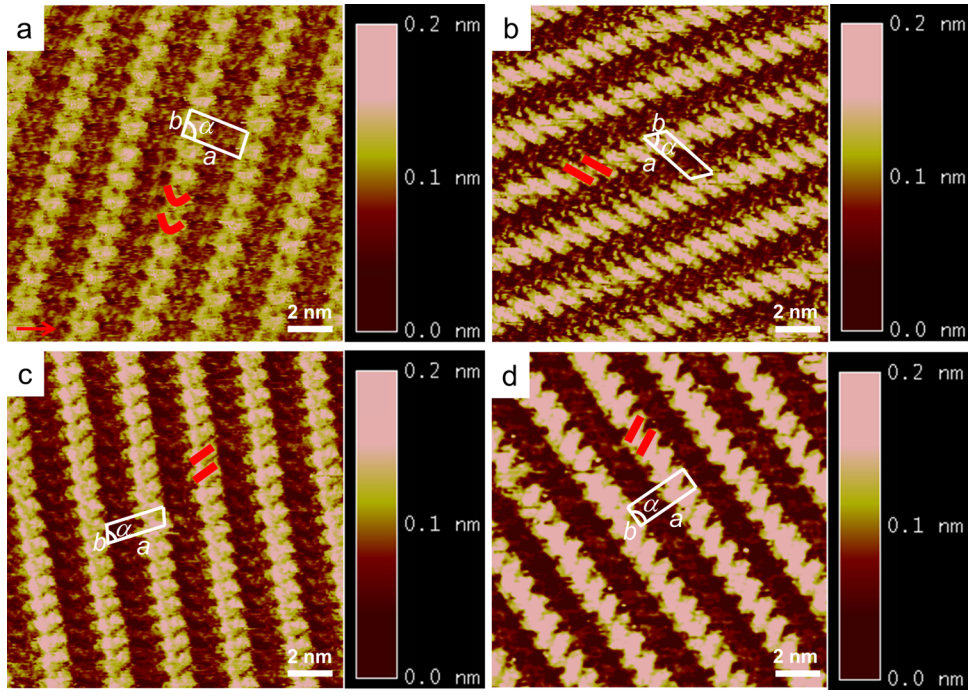

Figure 2. High-resolution STM images (15 nm × 15 nm) of molecule PAI1 (a), PAI2 (b), PAI6 (c), and PAI8 (d) at the 1-phenyloctane/HOPG interfaces. The unit cells are inserted on the STM images. Tunneling parameters: (a) 298.8 pA, 511.2 mV; (b) 299.1 pA, 567.3 mV; (c) 299.1 pA, 601.5 mV; and (d) 299.1 pA, 623.8 mV.

carboxyldiimide), PAI6 (*N*,*N*′-di(2-octyldodecyl)benzo[*c*]-picene-7,8,15,16-tetracarboxyldiimide), and PAI8 (*N*,*N*′-di(2-octyldodecyl)benzo[*c*]naphtho[2,1-*k*]tetraphene-5,6,14,15-tetracarboxyldiimide), as the target host molecules (Figure 1), which have the same alkyl chains but different backbone blocks.[31] The branched alkyl side chains attached on the imide nitrogen atoms help in ensuring the stable adsorption on the solid surface and the recognizable 2D structure. As a powerful tool to study the molecular systems adsorbed on flat and conductive solid substrates, scanning tunneling microscopy (STM) showed 2D self-assembled monolayers formed by PAI derivatives at the 1-phenyloctane/HOPG interface. Coronene molecules then periodically located on the specific highly ordered PAI1 host array. In combination with density functional theory (DFT) calculations, the results showed that coronene can only be immobilized in the bowl structure, whereas it is unstable on the planar PAI2, PAI6, and PAI8 monolayers. The formed Cor/PAI1 bilayer structure is more thermodynamically favorable than that of the PAI1 system. It is expected that systematic investigations may lead to control the distribution and dispersion of guest molecules on or in the preformed arrays on surface.

RESULTS AND DISCUSSION

Self-Assembled 2D Structure of PAIs. First, self-assemblies of four PAI derivatives were investigated. Figure 2 displays the high-resolution STM images of 2D molecular organizations. In each STM image, the brighter features

DOI: 10.1021/acsomega.7b00891
ACS Omega 2017, 2, 5611−5617

correspond to the conjugated backbone cores of the PAI derivatives, whereas the darker areas are occupied by the alkyl chains. The orientation of the backbones is parallel to each other, showing the formation of striped patterns. It is noteworthy that PAI1 exhibits bright "V"-shaped protrusion, indicating that the backbone of PAI1 is not parallel with respect to the substrate surface.[31−33] Such nonplanar geometry might be attributed to the distortion of the C-shaped polycyclic skeletons. The V-shaped configuration on the HOPG surface might come from the interaction between the interdigitated alkyl chains as well as the interaction between alkyl chains and the substrate. For PAI2, PAI6, and PAI8 molecules, they all exhibit rodlike protrusions in the STM images, indicating that their backbones are parallel to the HOPG surface. Therefore, the interactions between adsorbates and the substrate determine the stable adsorption of molecules on the surface. The unit cells containing one PAI molecule are superimposed on the STM images, and the unit-cell parameters are summarized in Table S1.

Although the distances between adjacent molecules are slightly different, there are great changes in the parameter α in the range of (82−99) ± 2°, indicating that the relative orientations of these PAI compounds are largely different. The orientation of the conjugated cores may be due to the hydrogen bond between −C═O and H−C of the phenyl ring from adjacent two molecules. One carbonyl group in PAI1 cannot form a hydrogen bond with the other adjacent PAI1 molecule because the neighboring backbone of PAI1 rotates out of the substrate surface. Additionally, the elastic alkyl chains tend to be out of the surface upon the close-packed surface.[34] In the cases of PAI2, PAI6, and PAI8, the carbonyl groups are on the two sides of the conjugated center; therefore, there might be two hydrogen bonds marked with red circles between two adjacent molecules. In these STM images, the widths of dark stripes are measured to be 1.2 ± 0.2 nm, which are consistent with the length of the alkyl side chains.

The molecular models (Figure 3) corresponding to STM images were obtained through DFT calculation, which further confirm the molecular geometry on the surface. The calculated interaction energies between adsorbates and interaction energies between adsorbates and the substrate in these systems are shown in Table 1. In these four systems, the interaction energies between adsorbates are around 20 kcal mol^{-1}, which result from the interactions between interdigitated alkyl chains. Compared with the other three systems, the slightly smaller intermolecular interaction in PAI1 might be attributed to the curled alkyl chain induced by the rotation of the backbone. The much larger interaction energies between adsorbates and substrates of PAI2, PAI6, and PAI8 than those of PAI1 are consistent with the supposed configuration of PAI1 above. The differences of adsorbate−substrate interaction energies between PAI2, PAI6, and PAI8 might be due to the backbones. These results provide evidence that the molecule−substrate interaction is the predominant factor relative to the molecule−molecule interaction. The low total energy per unit area in PAI1/HOPG systems compared to that of other systems supports the only inclusion of coronene molecules.

Selective Adsorption of Coronene on PAI1 Surface. Next, the coadsorption behavior of the guest coronene in these self-assembled patterns of PAI molecules was investigated. Except for the PAI1 monolayer, STM observation showed no evidence that the coronene molecule can be immobilized in other monolayers. In the large-scale STM image of coronene/PAI1, as shown in Figure S1, the stripes brighter than those of PAI1 were clearly visible, obviously indicating the localization of coronene molecules. The high-resolution STM image, as shown in Figure 4, shows that the V-shaped protrusion of PAI1 becomes circular spots. A unit cell is superimposed upon the STM image with a = 2.9 ± 0.1 nm, b = 1.3 ± 0.1 nm, and α = 99 ± 2°, which is significantly different from unit parameters of the parent PAI assembly (a = 2.7 ± 0.1 nm, b = 1.1 ± 0.1 nm, and α = 92 ± 2°). The width of the bright stripe is consistent with the diameter of the coronene plane parallel to the HOPG surface. The cross-sectional profiles (Figure 4b) show that the bright stripe is located higher than the darker stripe by around 0.1 nm in the PAI1 array, whereas the bright stripe is located higher than the darker stripe by around 0.2 nm after deposition of coronene. Additionally, competitive adsorption of coronene on the HOPG surface could not happen because there is no coronene phase, as has been observed. If coronene molecules preferentially adsorb on the HOPG surface, the structure of the PAI1 monolayer might be disturbed. From these factors, the adsorbed coronene molecule is expected to be located on the PAI1 conjugated cores.

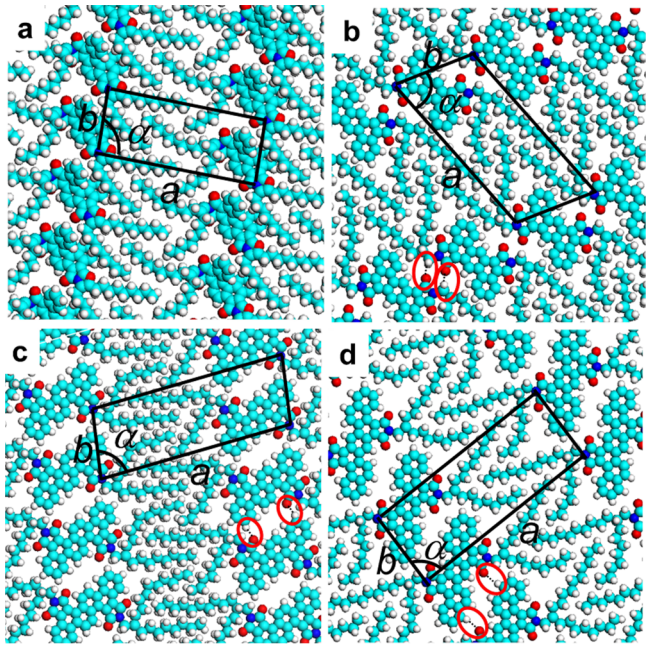

Figure 3. Molecular models (a)−(d) of self-assembled monolayers corresponding to the STM images (a)−(d) in Figure 2, respectively. The unit cells are inserted on the models.

The coronene and conjugated core of PAI1 cannot be resolved separately due to the limited resolution. The appropriate position of the coronene molecules can be identified by DFT calculation. The molecular model, as shown in Figure 4c, reveals the formation of a two-layer densely packed structure by specific adsorption of the coronene molecule on the bowl-conjugated core of PAI1. Coronene displayed parallel configuration to maximize the interaction between coronene and the substrate.[35] The interaction energies, including intermolecular and molecule−substrate, give more self-assembled information in the whole system, as summarized in Table 1. The contributions for the stable assembly of PAI compounds include the intermolecular interaction mainly coming from the interdigitated alkyl chains and the interaction between PAI1 and the substrate. After

DOI: 10.1021/acsomega.7b00891
ACS Omega 2017, 2, 5611−5617

Table 1. Calculated Interaction Energies in the Systems of PAI1/HOPG, PAI1 + Cor/HOPG, PAI2/HOPG, PAI6/HOPG, and PAI8/HOPG[a]

	interaction energies between adsorbates (kcal mol^{-1})	interaction energies between adsorbates and substrate (kcal mol^{-1})	total energy (kcal mol^{-1})	total energy per unit area (kcal mol^{-1} Å^{-2})
PAI1	−20.121	−56.286	−76.407	−0.237
PAI1 + Cor	−34.262	−133.794	−168.056	−0.458
PAI2	−21.712	−291.473	−314.185	−1.006
PAI6	−24.629	−332.837	−357.466	−1.058
PAI8	−23.966	−394.992	−418.958	−1.108

[a]Note that the more negative energy means the system is more stable.

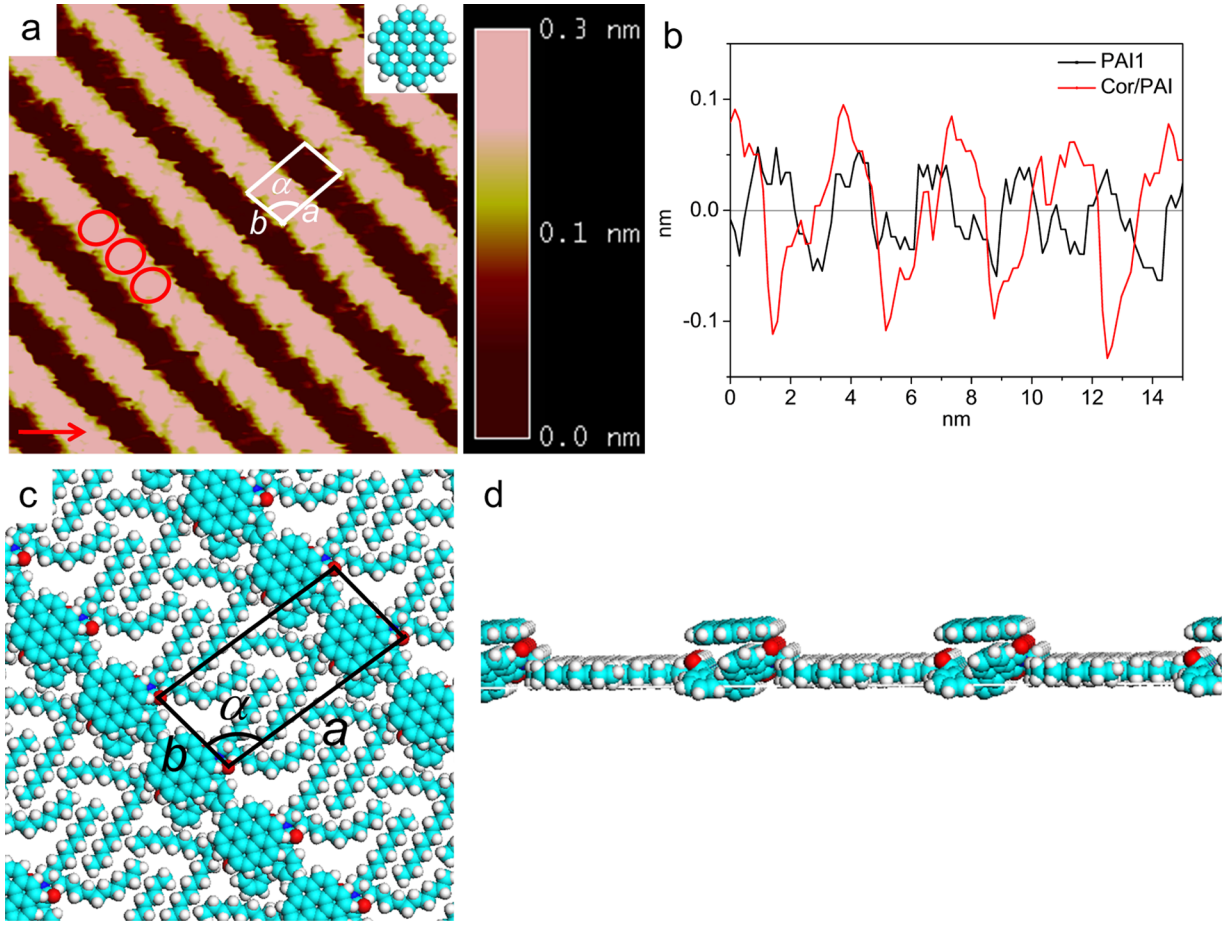

Figure 4. (a) High-resolution STM image of the self-assembled densely packed structure of Cor/PAI1/HOPG with the chemical structure of coronene (15 nm × 15 nm; I_{set} = 268.8 pA; V_{bias} = 580.4 mV), (b) line profile of the PAI1 and Cor/API1 monolayer on the HOPG surface corresponding to the STM images, (c) molecular model in image (a), (d) side view of the molecular model in (c).

addition of coronene molecules, the total intermolecular interaction energy, including that between PAI1 molecules and that between coronene and PAI1, was increased to −34.262 kcal mol^{-1}. This might be attributed to the interaction between the carboxyl oxygen atom and coronene. In other words, the interaction between coronene and PAI1 contributes to the location position of coronene. Note that the interaction energies between adsorbates and the substrate largely increase up to −133.794 kcal mol^{-1}, which indicates that there is a strong interaction between the coronene/PAI1 system and HOPG substrate. The adsorption of coronene molecules on PAI1 induced the increased stability of PAI1 on the HOPG substrate, leading to the increased interaction between PAI1 and the substrate. Therefore, the ordered coronene layer might be owing to the PAI1 layer and the HOPG underneath. On the monolayers of PAI2, PAI6, and PAI8, coronene molecules may tend to move because there is no groove structure to immobilize the molecules, resulting in that stable adsorption cannot be observed in STM images. In addition, DFT calculations showed smaller interaction energies for coronene on these monolayers, indicating that these are not preferable structures.

The total energy per unit area obtained through considering all possible interactions in the system offers an effective factor to evaluate the thermodynamic stability of different arrays. The selectivity of immobilization coronene in PAI1 can be explained by smaller total energy per unit area of PAI1 + Cor/HOPG (−0.458 kcal mol^{-1} Å^{-2}) system than that of PAI1/HOPG (−0.237 kcal mol^{-1} Å^{-2}), indicating the inclusion of coronene make the PAI1 monolayer more table. This function of stability

DOI: 10.1021/acsomega.7b00891
ACS Omega 2017, 2, 5611−5617

can be explained by the energy gain. The resulting interaction between physisorbed host and coronene with substrate overcomes the instability of the lower density of host matrix. In presence of coronene guest molecules, the formation of honeycomb network is thermodynamically favored.[6,7] As a result, the inclusion of coronene molecules in PAI1 monolayer should depend on the properties of molecular template monolayers.

To study the electronic interactions between the coronene molecules and PAI1 monolayer as well as the substrate, we also calculated the density of states (DOS) to discuss the energy level alignment at the coronene/PAI1 interface.[36,37] In Figure 5,

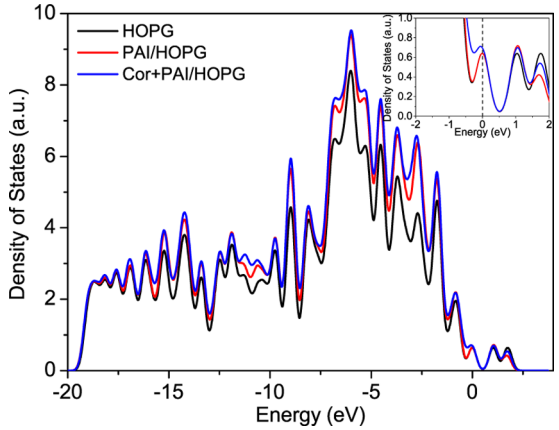

Figure 5. Density of states (DOS) for the HOPG slab and PAI/HOPG system before and after adsorption of coronene molecules. Fermi energy is aligned to 0 eV.

the DOS for PAI1/HOPG and Cor + PAI1/HOPG are shown. The increased total DOS structures indicate that strong interaction between coronene molecules and PAI1/HOPG system. The interaction between PAI1 and coronene molecule is calculated to be −22.717 kcal mol^{-1}. As shown in the enlarged DOS diagram, the adsorption of coronene molecules induced the change of energy-level alignment, which is expected to be used in organic electronics.

CONCLUSIONS

A series of PAI derivatives assembled into densely packed monolayers, in which only PAI1 can serve as a template for the immobilization of coronene molecules. In contrast to the spatial selection in the cavity, a close-packed coronene molecule atop the PAI1 monolayer has been observed. The selective incorporation of coronene is explained by the interaction energy on the basis of the theoretical calculations. Many systems for further symmetrical studies are needed to study the structures of templates which can adsorb coronene molecules, and it is necessary to further explore efficient recipes to distinguish clearly the specific position of guest molecules in the close-packed monolayer.

EXPERIMENTAL SECTION

Materials. The syntheses of PAI derivatives were carried out according to the previous report.[31] Self-assembled PAI monolayers were prepared by directly dropping the dilute solution of PAI derivative in 1-phenyloctane onto the freshly stripped HOPG (grade ZYB) surface, which was purchased from Agilent. The concentration of the solution was prepared to be less than 1.0×10^{-4} M to ensure the formation of highly ordered structures. The solution of coronene in 1-phenyloctane with the concentration of 1.0×10^{-2} M was prepared and then was directly dropped onto the PAI monolayer. After a while, a drop of 1-phenyloctane solution was deposited onto the preprepared surface followed by STM record.

Measurement. STM measurements were performed at the 1-phenyloctane/HOPG interface at room temperature (22−25 °C) by using a Nanoscope IIIa (Agilent) with tips mechanically formed from Pt/Ir (80/20). To obtain the topography image, constant-current STM was performed by continuously adjusting the vertical position of the STM tip. All of the tunneling conditions were given in the corresponding figure captions.

Calculations. Theoretical calculations were performed using the DFT-D scheme provided by DMol3 code.[38] We used the periodic boundary conditions (PBC) to describe the 2D periodic structure on the graphite in this work. The Perdew−Burke−Ernzerhof parameterization of the local exchange correlation energy was applied in local spin density approximation to describe exchange and correlation. All-electron spin-unrestricted Kohn−Sham wave functions were expanded on a local atomic orbital basis. For the large system, the numerical basis set was applied. All calculations were all-electron ones and performed with the medium mesh. The self-consistent field procedure was done with a convergence criterion of 10^{-5} au on the energy and electron density. Combined with the experimental data, we have optimized the unit-cell parameters and the geometry of the adsorbates in the unit cell. When the energy and density convergence criterion are reached, we could obtain the optimized parameters and the interaction energy between adsorbates. To evaluate the interaction between the adsorbates and HOPG, we design the model system. In our work, adsorbates consist of π-conjugated benzene rings. Because adsorption of benzene on graphite and graphene should be very similar, we have performed our calculations on infinite graphene monolayers using PBC. In the superlattice, graphene layers were separated by 35 Å in the normal direction. When modeling the adsorbates on graphene, we used graphene supercells and sampled the Brillouin zone by a $1 \times 1 \times 1$ k-point mesh. The interaction energy E_{inter} of adsorbates with graphite is given by $E_{inter} = E_{tot(adsorbates/graphene)} - E_{tot(isolated\ adsorbates\ in\ vacuum)} - E_{tot(graphene)}$. For the DOS calculations, k-point samplings for the Brillouin zone were performed using the $5 \times 5 \times 1$ Monkhorst−Pack k-point mesh.

ASSOCIATED CONTENT

Supporting Information

The Supporting Information is available free of charge on the ACS Publications website at DOI: 10.1021/acsomega.7b00891.

Experimental and calculated unit-cell parameters, large-scale STM images of PAI1 and PAI1/coronene structure (PDF)

AUTHOR INFORMATION

Corresponding Authors

*E-mail: tub@nanoctr.cn (B.T.).
*E-mail: dhzhao@pku.edu.cn (D.Z.).
*E-mail: zengqd@nanoctr.cn (Q.Z.).

ORCID

Dahui Zhao: 0000-0002-4983-4060
Qingdao Zeng: 0000-0003-3394-2232

DOI: 10.1021/acsomega.7b00891
ACS Omega 2017, 2, 5611−5617

Author Contributions

[§]Y.G. and S.W. equally contributed to this work.

Notes

The authors declare no competing financial interest.

■ ACKNOWLEDGMENTS

The authors are sincerely thankful to the support from the National Basic Research Program of China (2016YFA0200700) and National Natural Science Foundation of China (Nos. 21472029, 21773041, and 51473003).

■ REFERENCES

(1) De Feyter, S.; De Schryver, F. C. Two-dimensional supramolecular self-assembly probed by scanning tunneling microscopy. *Chem. Soc. Rev.* **2003**, *32*, 139−150.

(2) Tahara, K.; Furukawa, S.; Uji-i, H.; Uchino, T.; Ichikawa, T.; Zhang, J.; Mamdouh, W.; Sonoda, M.; De Schryver, F. C.; De Feyter, S.; Tobe, Y. Two-dimensional porous molecular networks of dehydrobenzo 12 annulene derivatives via alkyl chain interdigitation. *J. Am. Chem. Soc.* **2006**, *128*, 16613−16625.

(3) Kudernac, T.; Lei, S.; Elemans, J. A. A. W.; De Feyter, S. Two-dimensional supramolecular self-assembly: nanoporous networks on surfaces. *Chem. Soc. Rev.* **2009**, *38*, 402−421.

(4) Blunt, M. O.; Russell, J. C.; Gimenez-Lopez, M. D.; Taleb, N.; Lin, X. L.; Schroder, M.; Champness, N. R.; Beton, P. H. Guest-induced growth of a surface-based supramolecular bilayer. *Nat. Chem.* **2011**, *3*, 74−78.

(5) Yoshimoto, S.; Tsutsumi, E.; Narita, R.; Murata, Y.; Murata, M.; Fujiwara, K.; Komatsu, K.; Ito, O.; Itaya, K. Epitaxial supramolecular assembly of fullerenes formed by using a coronene template on a Au(111) surface in solution. *J. Am. Chem. Soc.* **2007**, *129*, 4366−4376.

(6) Furukawa, S.; Tahara, K.; De Schryver, F. C.; Van der Auweraer, M.; Tobe, Y.; De Feyter, S. Structural transformation of a two-dimensional molecular network in response to selective guest inclusion. *Angew. Chem., Int. Ed.* **2007**, *46*, 2831−2834.

(7) Blunt, M.; Lin, X.; Gimenez-Lopez, M. D.; Schroder, M.; Champness, N. R.; Beton, P. H. Directing two-dimensional molecular crystallization using guest templates. *Chem. Commun.* **2008**, 2304−2306.

(8) Hietschold, M.; Lackinger, M.; Griessl, S.; Heckl, W. M.; Gopakumar, T. G.; Flynn, G. W. Molecular structures on crystalline metallic surfaces - From STM images to molecular electronics. *Microelectron. Eng.* **2005**, *82*, 207−214.

(9) Yoshimoto, S.; Tsutsumi, E.; Fujii, O.; Narita, R.; Itaya, K. Effect of underlying coronene and perylene adlayers for 60 fullerene molecular assembly. *Chem. Commun.* **2005**, 1188−1190.

(10) Walzer, K.; Sternberg, M.; Hietschold, M. Formation and characterization of coronene monolayers on HOPG(0001) and MoS2(0001): a combined STM/STS and tight-binding study. *Surf. Sci.* **1998**, *415*, 376−384.

(11) Gyarfas, B. J.; Wiggins, B.; Zosel, M.; Hipps, K. W. Supramolecular structures of coronene and alkane acids at the Au(111)-solution interface: A scanning tunneling microscopy study. *Langmuir* **2005**, *21*, 919−923.

(12) Zhang, H.-X.; Chen, Q.; Wen, R.; Hu, J.-S.; Wan, L.-J. Effect of polycyclic aromatic hydrocarbons on detection sensitivity of ultratrace nitroaromatic compounds. *Anal. Chem.* **2007**, *79*, 2179−2183.

(13) Gong, J. R.; Yan, H. J.; Yuan, Q. H.; Xu, L. P.; Bo, Z. S.; Wan, L. J. Controllable distribution of single molecules and peptides within oligomer template investigated by STM. *J. Am. Chem. Soc.* **2006**, *128*, 12384−12385.

(14) Lu, J.; Lei, S. B.; Zeng, Q. D.; Kang, S. Z.; Wang, C.; Wan, L. J.; Bai, C. L. Template-induced inclusion structures with copper(II) phthalocyanine and coronene as guests in two-dimensional hydrogen-bonded host networks. *J. Phys. Chem. B* **2004**, *108*, 5161−5165.

(15) Griessl, S. J. H.; Lackinger, M.; Jamitzky, F.; Markert, T.; Hietschold, M.; Heckl, W. A. Incorporation and manipulation of coronene in an organic template structure. *Langmuir* **2004**, *20*, 9403−9407.

(16) Xue, J.; Deng, K.; Liu, B.; Duan, W.; Zeng, Q.; Wang, C. Site-selection and adaptive reconstruction in a two-dimensional nanoporous network in response to guest inclusion. *RSC Adv.* **2015**, *5*, 39291−39294.

(17) Zhang, S.; Zhang, J.; Deng, K.; Xie, J.; Duan, W.; Zeng, Q. Solution concentration controlled self-assembling structure with host-guest recognition at the liquid-solid interface. *Phys. Chem. Chem. Phys.* **2015**, *17*, 24462−24467.

(18) Dai, H.; Yi, W.; Deng, K.; Wang, H.; Zeng, Q. Formation of Coronene Clusters in Concentration and Temperature Controlled Two-Dimensional Porous Network. *ACS Appl. Mater. Interfaces* **2016**, *8*, 21095−21100.

(19) Shen, M.; Luo, Z.; Zhang, S.; Wang, S.; Cao, L.; Geng, Y.; Deng, K.; Zhao, D.; Duan, W.; Zeng, Q. A size, shape and concentration controlled self-assembling structure with host-guest recognition at the liquid-solid interface studied by STM. *Nanoscale* **2016**, *8*, 11962−11968.

(20) Schull, G.; Douillard, L.; Fiorini-Debuisschert, C.; Charra, F.; Mathevet, F.; Kreher, D.; Attias, A. J. Selectivity of single-molecule dynamics in 2D molecular sieves. *Adv. Mater.* **2006**, *18*, 2954−2957.

(21) Schull, G.; Douillard, L.; Fiorini-Debuisschert, C.; Charra, F.; Mathevet, F.; Kreher, D.; Attias, A. J. Single-molecule dynamics in a self-assembled 2D molecular sieve. *Nano Lett.* **2006**, *6*, 1360−1363.

(22) Wu, D.; Deng, K.; He, M.; Zeng, Q.; Wang, C. Coadsorption-induced reconstruction of supramolecular assembly characteristics. *ChemPhysChem* **2007**, *8*, 1519−1523.

(23) Liu, J.; Zhang, X.; Yan, H. J.; Wang, D.; Wang, J. Y.; Pei, J.; Wan, L.-J. Solvent-Controlled 2D Host-Guest (2,7,12-Trihexyloxytruxene/Coronene) Molecular Nanostructures at Organic Liquid/Solid Interface Investigated by Scanning Tunneling Microscopy. *Langmuir* **2010**, *26*, 8195−8200.

(24) Eder, G.; Kloft, S.; Martsinovich, N.; Mahata, K.; Schmittel, M.; Heckl, W. M.; Lackinger, M. Incorporation Dynamics of Molecular Guests into Two-Dimensional Supramolecular Host Networks at the Liquid-Solid Interface. *Langmuir* **2011**, *27*, 13563−13571.

(25) MacLeod, J. M.; Ben Chaouch, Z.; Perepichka, D. F.; Rosei, F. Two-Dimensional Self-Assembly of a Symmetry-Reduced Tricarboxylic Acid. *Langmuir* **2013**, *29*, 7318−7324.

(26) Huang, W.; Zhao, T. Y.; Wen, M. W.; Yang, Z. Y.; Xu, W.; Yi, Y. P.; Xu, L. P.; Wang, Z. X.; Gu, Z. J. Ad layer Structure of Shape-Persistent Macrocycle Molecules: Fabrication and Tuning Investigated with Scanning Tunneling Microscopy. *J. Phys. Chem. C* **2014**, *118*, 6767−6772.

(27) Tahara, K.; Nakatani, K.; Iritani, K.; De Feyter, S.; Tobe, Y. Periodic Functionalization of Surface-Confined Pores in a Two-Dimensional Porous Network Using a Tailored Molecular Building Block. *ACS Nano* **2016**, *10*, 2113−2120.

(28) Martínez-Blanco, J.; Mascaraque, A.; Dedkov, Y. S.; Horn, K. Ge(001) As a Template for Long-Range Assembly of pi-Stacked Coronene Rows. *Langmuir* **2012**, *28*, 3840−3844.

(29) Martínez-Blanco, J.; Walter, B.; Mascaraque, A.; Horn, K. Long-Range Order in an Organic Over layer Induced by Surface Reconstruction: Coronene on Ge(111). *J. Phys. Chem. C* **2014**, *118*, 11699−11703.

(30) Zhang, R.; Wang, L. C.; Li, M.; Zhang, X. M.; Li, Y. B.; Shen, Y. T.; Zheng, Q. Y.; Zeng, Q. D.; Wang, C. Heterogeneous bilayer molecular structure at a liquid-solid interface. *Nanoscale* **2011**, *3*, 3755−3759.

(31) Wang, R. R.; Shi, K.; Cai, K.; Guo, Y. K.; Yang, X.; Wang, J. Y.; Pei, J.; Zhao, D. H. Syntheses of polycyclic aromatic diimides via intramolecular cyclization of maleic acid derivatives. *New J. Chem.* **2016**, *40*, 113−121.

(32) Zhang, X.; Li, S. S.; Lin, H.; Wang, D.; Xu, W.; Wan, L. J.; Zhu, D. B. Molecular adlayer and photo-induced structural transformation of a diarylethene derivative on Au(111) investigated with scanning tunneling microscopy. *J. Electroanal. Chem.* **2011**, *656*, 304−311.

DOI: 10.1021/acsomega.7b00891
ACS Omega 2017, 2, 5611−5617

(33) Chen, J. D.; Lu, H. Y.; Chen, C. F. Synthesis and Structures of Multifunctionalized Helicenes and Dehydrohelicenes: An Efficient Route to Construct Cyan Fluorescent Molecules. *Chem. − Eur. J.* **2010**, *16*, 11843−11846.
(34) Cun, H.; Wang, Y. L.; Du, S. X.; Zhang, L.; Zhang, L. Z.; Yang, B.; He, X. B.; Wang, Y.; Zhu, X. Y.; Yuan, Q. Z.; Zhao, Y. P.; Ouyang, M.; Hofer, W. A.; Pennycook, S. J.; Gao, H. J. Tuning Structural and Mechanical Properties of Two-Dimensional Molecular Crystals: The Roles of Carbon Side Chains. *Nano Lett.* **2012**, *12*, 1229−1234.
(35) Richardson, N. V. Adsorption-induced chirality in highly symmetric hydrocarbon molecules: lattice matching to substrates of lower symmetry. *New J. Phys.* **2007**, *9*, 395.
(36) Godlewski, S.; Tekiel, A.; Piskorz, W.; Zasada, F.; Prauzner-Bechcicki, J. S.; Sojka, Z.; Szymonski, M. Supramolecular Ordering of PTCDA Molecules: The Key Role of Dispersion Forces in an Unusual Transition from Physisorbed into Chemisorbed State. *ACS Nano* **2012**, *6*, 8536−8545.
(37) Chilukuri, B.; Mazur, U.; Hipps, K. W. Effect of dispersion on surface interactions of cobalt(II) octaethylporphyrin monolayer on Au(111) and HOPG(0001) substrates: a comparative first principles study (vol 16, pg 14096, 2014). *Phys. Chem. Chem. Phys.* **2014**, *16*, 20250.
(38) Perdew, J. P.; Burke, K.; Ernzerhof, M. Generalized gradient approximation made simple. *Phys. Rev. Lett.* **1996**, *77*, 3865−3868.

DOI: 10.1021/acsomega.7b00891
ACS Omega 2017, 2, 5611−5617